Chapter 6

Effects of High-Density Oxygen Plasma Post-treatment on the Field Emission Characteristics of Carbon-Nanotube Field-Emission Displays

The effects of oxygen plasma post-treatment (PPT) on the morphology and field emission properties of carbon nanotube (CNT) arrays grown on silicon substrates are proposed and experimental results are reported. Oxygen PPT led to an enhancement in the emission properties of CNTs, which showed an increase in total emission current density and a decrease in turn-on field after plasma treatment. Scanning electron microscopy (SEM) images showed reduced densities of the CNTs, which resulted in a decrease of the screening effect in the electric field. Raman spectra showed an increase in the number of defects which served as field-emission sites when the plasma power or treatment time with the plasma increased. Transmission electron microscopy (TEM) images were used to identify the quality of the nanotubes, so that we could clearly find evidences of improvement in the field emission properties after plasma treatment. The measurement of electrical characteristics revealed improved field emission properties under proper plasma conditions. The turn-on field decreased from 4.8 to 2.5 V/μm, and the emission current density increased from 78.7 μ A/cm^2 to 18mA/cm^2 at an applied field of 5.5

V/μm. Besides, the threshold field is about 4.92 V/μm with 250 W and 90s oxygen plasma post-treatment.

6.1 Introduction

Carbon nanotubes (CNTs) have attracted a great deal of interest for their remarkable properties, such as their high aspect ratio, high mechanical strength, chemical stability, super-thermal conductivity, and electron emission properties [6.1-6.2]. Because CNTs exhibit extremely high electron emission currents at low operating voltages due to their high aspect ratio, CNTs have been regarded as a strong candidate for field-emission displays. The density of CNTs plays a crucial role in their field emission properties. For film with high CNT density, the screening effect reduces the field enhancement and thus reduces the emitted current. Therefore, it is important to control the density of CNTs in field emission applications. However, the density of CNTs grown by MPCVD still cannot be controlled effectively. The effect of screening electric field by the dense arrangement of CNTs has been reported by several groups [6.3-6.5]. The density of CNTs determines the emission site density (ESD). If the CNTs are too closely spaced, the electric field is screened out. Groning *et al.*[6.5] reported that the field enhancement factor β of the tips decreases rapidly when the inter-tip spacing is smaller than twice the length of the tips. For a larger spacing, the current density decreases due to the decreasing

density of the tips. For a smaller spacing, the current density decreases rapidly due to the decreasing β factor, and this effect cannot be compensated for by increasing the density of the emitting tips. This shows that when the spacing between the emitting structures on a surface becomes comparable to their length, problems of shielding occur that limit the emission current density.

Recently, plasma post-treatment has been used to etch the surface of CNTs and change the density of CNTs. Plasma post-treatment has several effects. First, it changes the structure of carbon nanotubes on their walls and tips. Second, it purifies the carbon nanotubes by eliminating amorphous carbon. Third, it changes the density of CNTs and causes defects on CNTs. Therefore, to optimize the density of CNTs and to obtain better field emission properties, proper plasma post-treatments on CNTs are needed. Several plasma post-treatment methods [6.6-6.9] including the use of H_2, Ar and CF_4 plasma were reported to improve the field emission properties of CNTs, but these methods do not improve the field emission properties very well. In this study, we use high-density oxygen plasma in Inductively Coupled Plasma reactive ion etching (ICP-RIE) to modify the density of CNTs grown by microwave plasma chemical vapor deposition (MPCVD), which causes many defects on CNTs. Different plasma power densities and plasma etching times were utilized to obtain various CNT morphologies. The experimental results reveal improved field

emission properties under proper plasma conditions. The turn-on field decreased from 4.8 to 2.5 V/μm, and the emission current density increased from 78.7 μ A/cm^2 to 18mA/cm^2 at an applied field of 5.5 V/μm.

6.2 Experimental Procedures

In this study, the fabrication procedures for CNTs treated with plasma post-treatment are shown schematically in Figs. 6-1(a) – 6-1(f). As shown in Fig. 6-1(b), a 1-μm-thick photoresist was spin-coated on an n-type Si(100) substrate, and square cells with an emission area 1.5 mm^2 were patterned by photolithography, as shown in Fig. 6-1(b). Then a thin Fe layer (~3.5 nm) was deposited directly on the photoresist patterned Si substrate by electron beam evaporation, as shown in Fig. 6-1(c). Fe patterns were formed after the photoresist was removed by the lift-off method as depicted in Fig. 6-1(d). Finally, carbon nanotubes were grown selectively on the Fe patterns by microwave plasma enhanced chemical vapor deposition (MPECVD) as shown in Fig. 6-1(e). CH_4 and H_2 were used as the source gases and the typical flow rates were 5 and 100 sccm, respectively. The microwave power was kept at 1.2 kW and the chamber pressure was held at 30 Torr. The hydrogen plasma was introduced first to change the Fe layer into Fe nanoparticles. Then CH_4 was decomposed in the hydrogen plasma and transition metals adsorbed carbon atoms to form nanotubes. The substrate temperature during growth was estimated to be

700℃ and the growth time was 5 min. CNTs were formed by the post-plasma treatment in an ICP-RIE system, as shown in Fig. 6-1(f). The pressure in the ICP-RIE system was 10mTorr and the oxygen flow rate was 40sccm. The density of carbon nanotubes was modified by ICP RF power and plasma etching time.

A high-vacuum measuring environment was established to characterize the field emission properties of the carbon nanotubes. The vacuum chamber was evacuated using a turbo pump. Cathode contact was made directly on the wafer. The anode plate was a glass plate coated with an ITO layer and a P22 phosphor. All cables were shielded except for the ground return path to the power source. The DC measurement system was based on Keithley 237 high-voltage source units with an IEEE 488 interface. The measurement instruments were auto-controlled by a computer. During the measurement, the space between the emitter (cathode) and anode was controlled to be approximately at 190 um and the base pressure in the testing chamber was approximately 1.0×10^{-6} Torr. The field emission characterization of the CNT films was measured with a voltage sweep from 0 V to 1100 V and the emission area of the CNT films was 1.5 mm^2.

6.3 Results and Discussion

Figure 6-2 shows the typical top view SEM images and cross-sectional views of CNT films before and after O_2 plasma treatment. The O_2 gas flow rate was

40sccm and the etching time was 60 s with different ICP powers: (a) untreated, (b) 250 W, (c) 400 W and (d) 600 W. The density of the CNTs decreases as plasma power increases, which results from the destruction of CNTs during oxygen plasma treatment. For the untreated case, the CNTs were aligned and closely spaced, the length of CNTs was approximately 20 um and the density of the CNT film is very high. The reason for the aligned nanotube growth is the high density of CNTs grown from the densely packed catalytic nanoparticles. As the nanotubes lengthen, the interaction between nanotubes by Van der Waals force forms a large bundle with some rigidity, which enables THE CNTs to continue growing in the same direction. For a plasma power of 250 W, parts of the CNTs were destroyed by O_2 plasma, and variation in the length of CNTs increased. From the SEM image, the CNTs on the substrate tend to cluster together to form bundles. Carbon nanotubes and amorphous carbon can be seen in the SEM image. For a plasma power of 400 W, most of the CNTs were destroyed by O_2 plasma except for a few curled nanotubes lying on the substrate. For a plasma power of 600 W, almost all CNTs were destroyed obviously except for amorphous carbon or carbon particles existing on the substrate and field emission phenomenon was not observed in the Fowler-Nordheim plot.

Figure 6-3 shows the SEM images of CNTs treated by O_2 plasma at a power of 400 W with different etching times. For the case of 30 s [Fig. 6-3(a)], the length and

the density of the CNTs were not clearly changed. The CNTs on the substrate tend to cluster together to form bundles. Carbon nanotubes and amorphous carbon can be seen from the SEM image. In the case of 60 s [Fig. 6-3(b)], most CNTs were destroyed by the plasma. In the case of 90 s [Fig. 6-3(c)], almost none of the CNTs exist and only amorphous carbon or carbon particles are present. Similar results were found in the case of an O_2 plasma power of 250 W with different etching times.

To investigate crystallization and defects in CNTs post-treated in high-density O_2 plasma, Raman spectroscopy and transmission electron microscopy (TEM) were used. The results are shown from Figs. 6-4 to 6-6. All the spectra (Figs. 6-4 and 6-5) clearly show two sharp peaks at approximately 1350 cm^{-1}(D band) and 1596 cm^{-1}(G band). Raman spectra indicate the difference in peak density and width according to various plasma post-treatment times and various plasma powers. The strong intensity at approximately 1350 cm^{-1} (D band) indicates disorder and defects in CNTs, and the peak at approximately 1596 cm^{-1} (G band) indicates highly oriented pyrolytic graphite[6.10-6.11]. Figures 6-4 and 6-5 show an increase in intensity ratio (I_D/I_G) when plasma treatment time or plasma power increases. Because oxygen can easily react with carbon and plasma ions bombarded on CNTs, it may be suggested that the increase in I_D/I_G was caused by disorder and defects in CNTs caused by O_2

plasma etching effects. In order to further identify the quality of nanotubes treated by plasma, TEM was used. Figure 6-6 shows TEM images of CNTs (a) before and (b) after O_2 plasma post-treatment. The plasma power and treatment time is 400 W and 60s, respectively. Figure 6-6(a) shows a high resolution TEM image of CNTs without plasma treatment. Catalytic nanoparticles existed at the roots of nanotube and well-structured graphite sheets parallel to the tube axis were observed. The inset in Fig. 6-6(a) reveals that nanotubes grown by MPCVD have a peculiar bamboolike shape. Figure 6-6(b) shows a TEM image of CNTs treated by plasma. The graphite structure of outer walls of the nanotubes seems to be destroyed by the plasma, and the tips of the nanotubes seem to be sharpened by the plasma. Structural defects were proved to be emission sites by Chen et al. [6.12] and sharpened tips (the aspect ratio is high) seemed to easily emit electrons because of further increments in the local electric field. Therefore, the defects and sharpened tips of nanotubes formed by plasma treatment are the main possible causes of the improved field emission properties of nanotubes after plasma treatment.

The field emission characteristics and the corresponding F-N plots for CNTs after plasma treatment under different conditions are shown from Figs.6-7 to 6-9. Here the turn-on field is defined as the field at which an emission current density of 1 μ A/cm^2 is generated. In Fig. 6-7, the plasma post-treatment time is fixed at 60 s.

The field emission current densities increased from 78.7 μ A/cm^2 to 8mA/cm^2 when the applied field was 5.5 V/μm for the untreated and 400 W plasma post-treatment, respectively. The turn-on field decreased from 4.8 to 2.9 V/μm for the untreated and 400 W plasma post-treatment, respectively. Possible explanations for this result are as follows. In the case of non-plasma post-treatment, the density of the CNTs is very high. Therefore, the field screening effect is serious and has a high turn-on electric field and a low field emission current density. However, in the cases of 250 W and 400 W plasma powers with plasma treatment times fixed at 60 s, O_2 plasma can destroy the structure of the CNTs so that the morphology of CNT film is less dense and the field screening effect is not as serious. The turn-on field is about the same for the 250 W and 400 W plasma power cases, but the current density at 5.5 V/μm for the 400 W plasma power case is 3 mA/cm^2 higher than that for the 250 W plasma power case. The defects and sharpened tips produced by plasma may explain this result. The defects and sharpened tips of CNTs produced by higher-plasma-power post-treatment are much more pronounced than for lower plasma power post treatment. Therefore, a large number of structural defects exist on the surface of the nanotubes as well as on their tips. These defects also serve as emission sites for increasing the total emission current. In addition, those sharpened tips can emit electrons easily due to their high aspect ratio. Thus, we can achieve a

higher emission current density by higher-plasma-power post-treatment. However, in the case of 600 W-plasma-power post-treatment, the CNTs are almost destroyed by plasma and thus no field emission phenomenon is observed. The corresponding FN plots of nanotubes for different plasma power treatments for a 60 s treatment time are shown in Fig. 6-7(b). The linearity confirms the field emission property of the fabricated devices.

In Fig. 6-8, the plasma power is fixed at 400 W and the treatment time is 30 s, 60 s and 90 s. In the case of 30 s plasma post-treatment time, the density of the CNTs does not change obviously. Therefore, the turn-on field does not improve compared with the untreated case. As for the 90 s case, the CNTs are almost destroyed by plasma except for a few nanotubes still existing on the substrate. Therefore, we cannot obtain good field emission properties. Due to proper plasma treatment, we can achieve a lower density of CNTs with more defects and sharpened tips, which also serve as field emission sites. Therefore, a low turn-on field (2.9 V/μm) and a high field emission current density (8mA/cm^2) are obtained in the case of a 60 s plasma treatment.

In Fig. 6-9, the plasma power is fixed at 250 W and the plasma treatment time is 30 s, 60 s and 90 s. The turn-on electrical field of the CNT field emission array decreases from 4.8 to 2.5 V/μm for the untreated CNTs and the PPT-CNTs

with a plasma power of 250 W and an etching time of 90 s, respectively. The field emission current density increased from 78.7 μA/cm^2 to 18mA/cm^2 at an electric field of 5.5 V/μm. The possible explanations of these improved results are as follows. The reduced turn-on field is primary due to the reduced density of CNTs because of O_2 plasma post-treatment. The better field emission current density (18mA/cm^2) at an electric field of 5.5 V/μm may be due to the large number of emitting sites still existing on the nanotubes. Defects and sharpened tips produced by plasma serving as field-emitting sites are another source for the high emission current density. Figure 6-10 shows the stability of electron emission of nanotubes after plasma treatment at a 650 V anode voltage for 1500 s. The emission current fluctuation was about ± 13% within 1500 s. The PPT-CNTs seemed to exhibit current fluctuation due to some of the electrons emitted from defects produced by plasma treatment. Table 6-1 summarizes the field emission properties of the CNTs for different conditions of plasma post- treatment

6.4 Conclusions

Modifying the surface morphology of CNTs has been achieved by oxygen plasma post-treatments. SEM images revealed reduced densities of CNTs after O_2 plasma post-treatment. Raman spectra showed an increase in the number of defects

which served as field-emission sites when the plasma power or treatment time with plasma increased. Transmission electron microscopy (TEM) images were used to identify the quality of nanotubes so that we could clearly find evidences of improvement in the field emission properties after plasma treatment. The field emission characteristics confirmed the improvement of field emission properties under proper PPT conditions. The turn-on electric field decreased from 4.8 to 2.5 V/μm for untreated and PPT conditions of a plasma power of 250 W and an etching time of 90 s, respectively, and the field emission current density increased from 78.7 μA/cm^2 to 18 mA/cm^2 at an electric field of 5.5 V/μm. Besides, the threshold field is about 4.92 V/μm with 250 W and 90s oxygen plasma post-treatment.

The experimental results reveal that improved emission properties can be achieved by optimizing the density of CNTs and the defects on nanotubes produced by plasma under proper plasma treatment conditions.

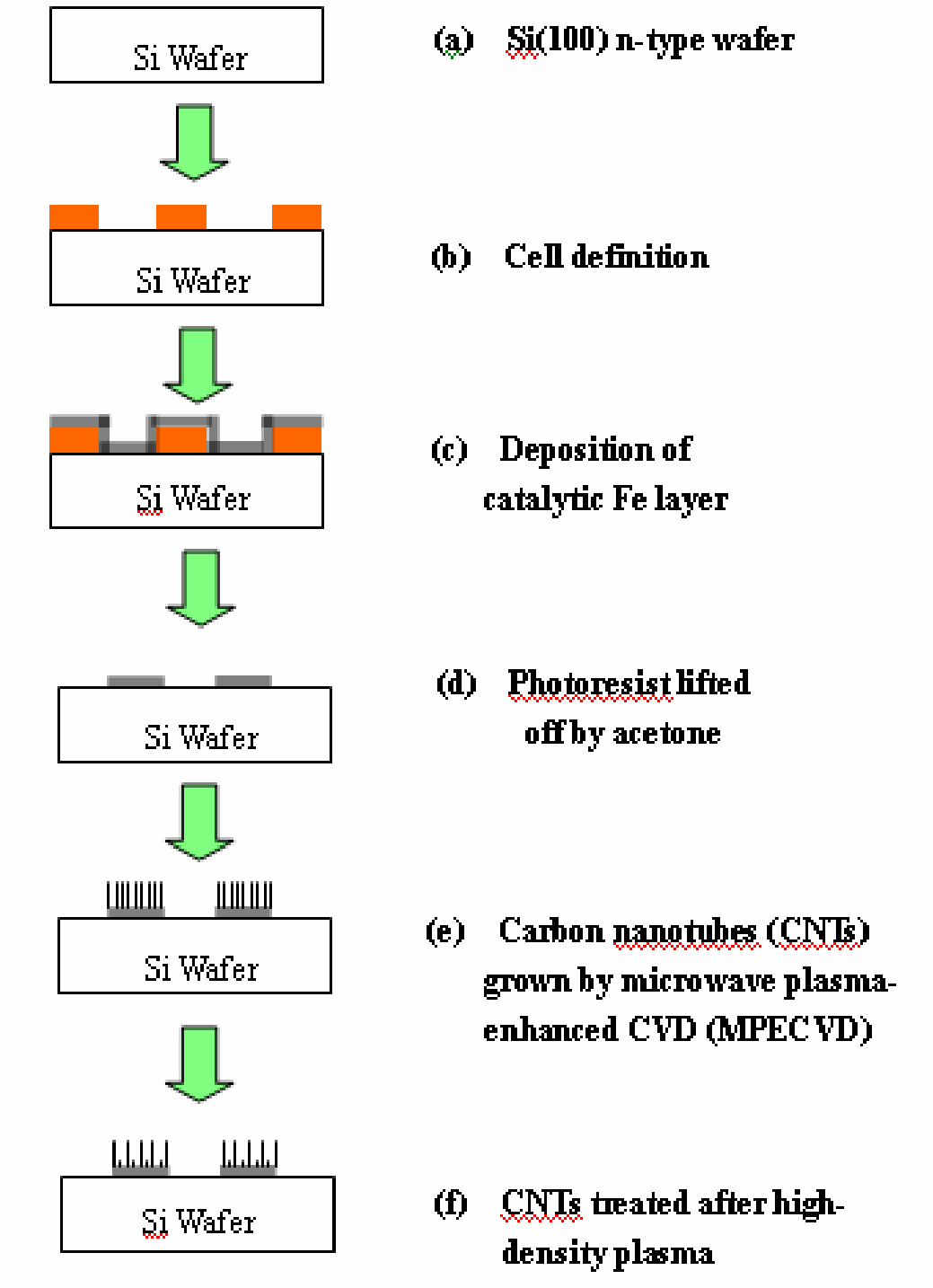

Figure 6-1 Fabrication procedures for CNTs treated by O_2 plasma etching.

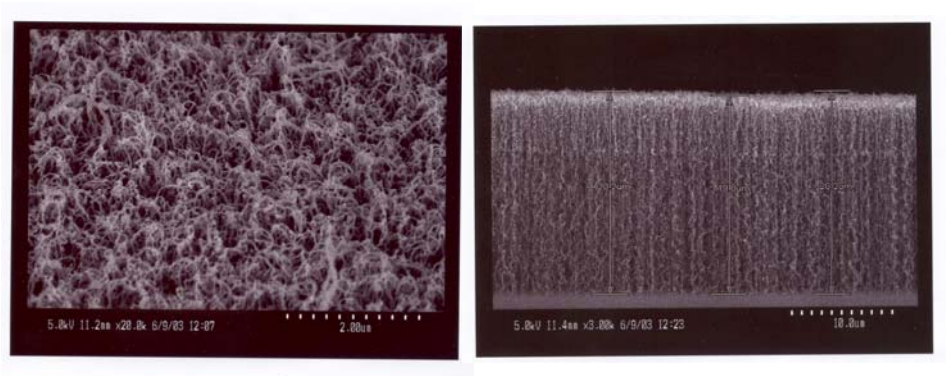

(a)

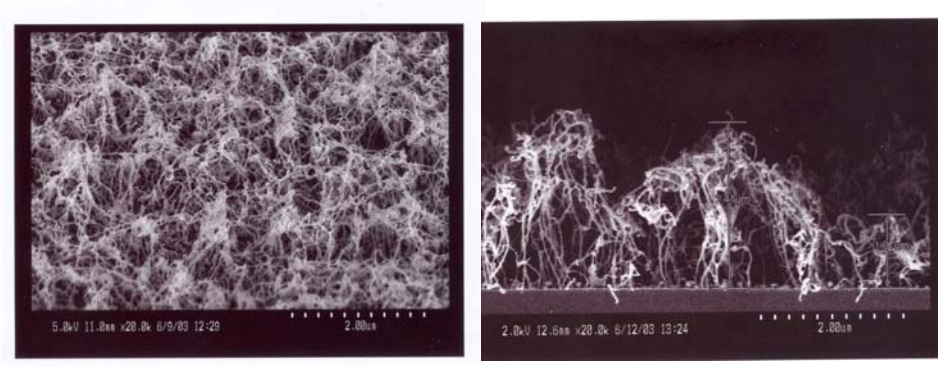

(b)

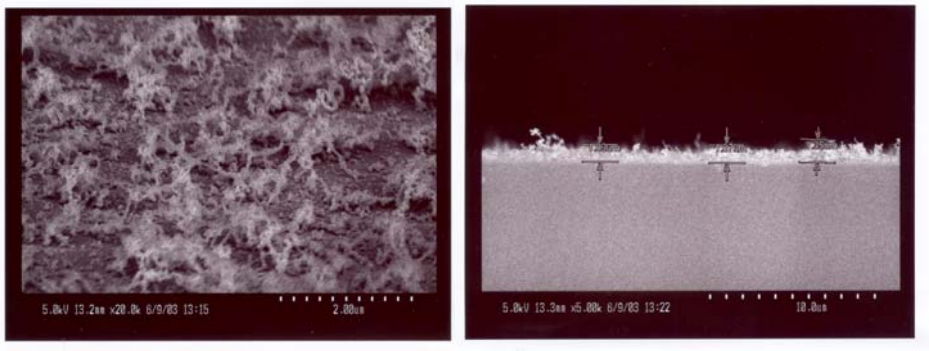

(c)

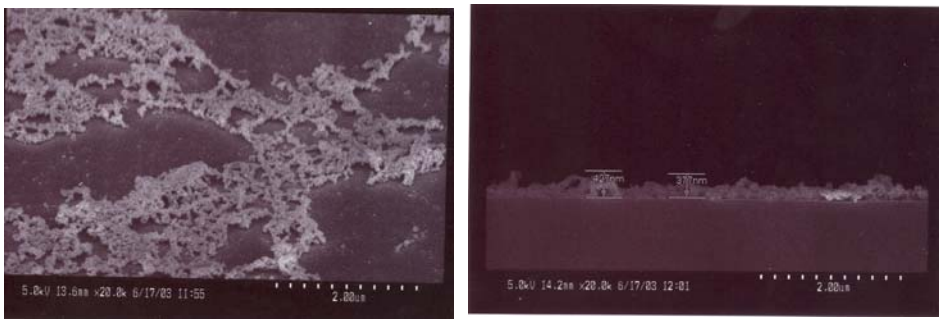

(d)

Figure 6-2 SEM images of CNTs treated with 60 s O_2 PPT for different ICP powers of (a) non-PPT, (b) 250 W, (c) 400 W and (d) 600 W.

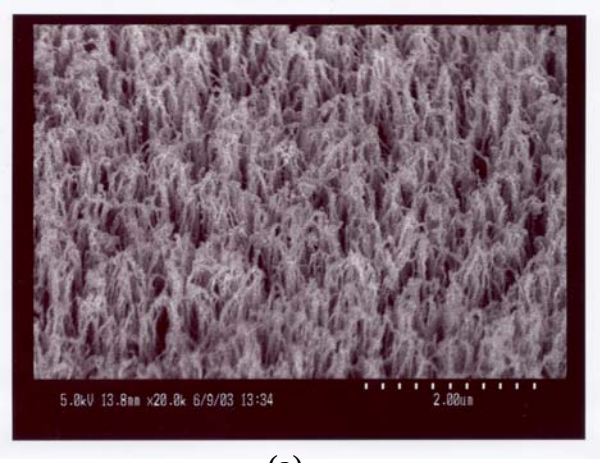

(a)

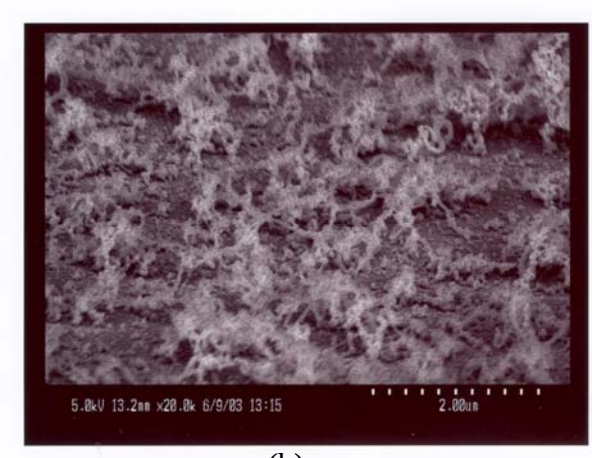

(b)

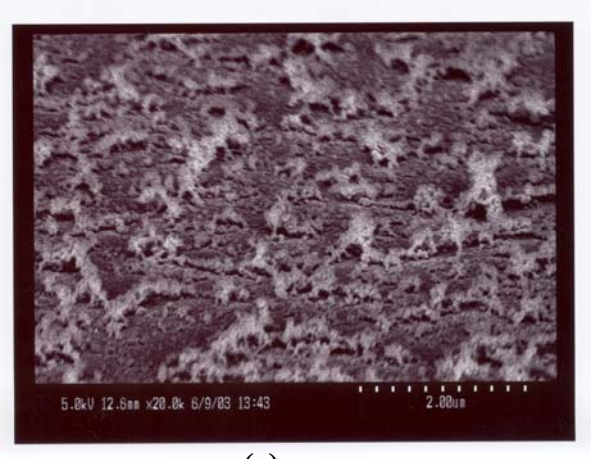

(c)

Figure 6-3 SEM images of CNTs treated by PPT for different ICP plasma etching times (a) 30 s, (b) 60 s and (c) 90 s. The ICP plasma power was held at 400 W.

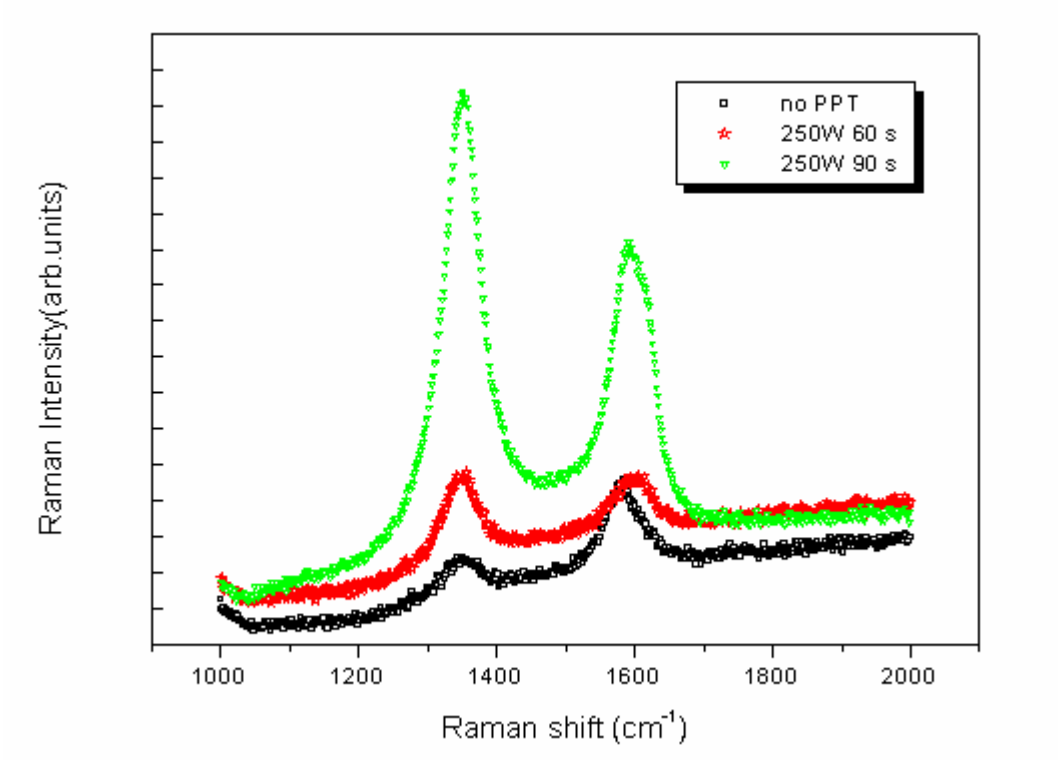

Figure 6-4 Raman spectra of CNTs under various lengths of O_2 plasma post-treatment.

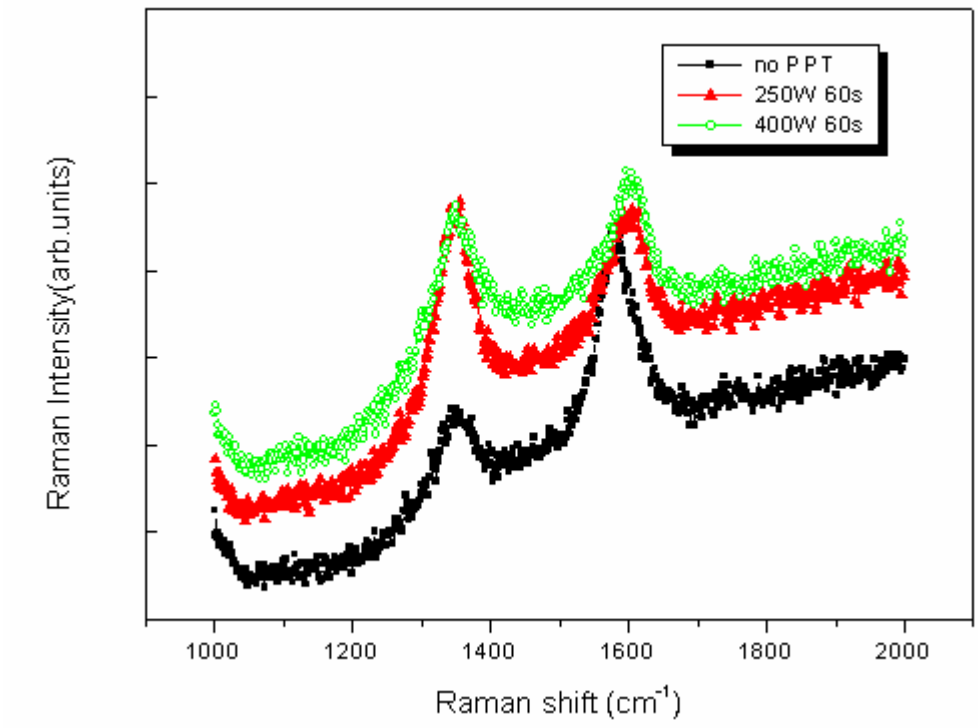

Figure 6-5 Raman spectra of CNTs under O_2 plasma post-treatment at various powers.

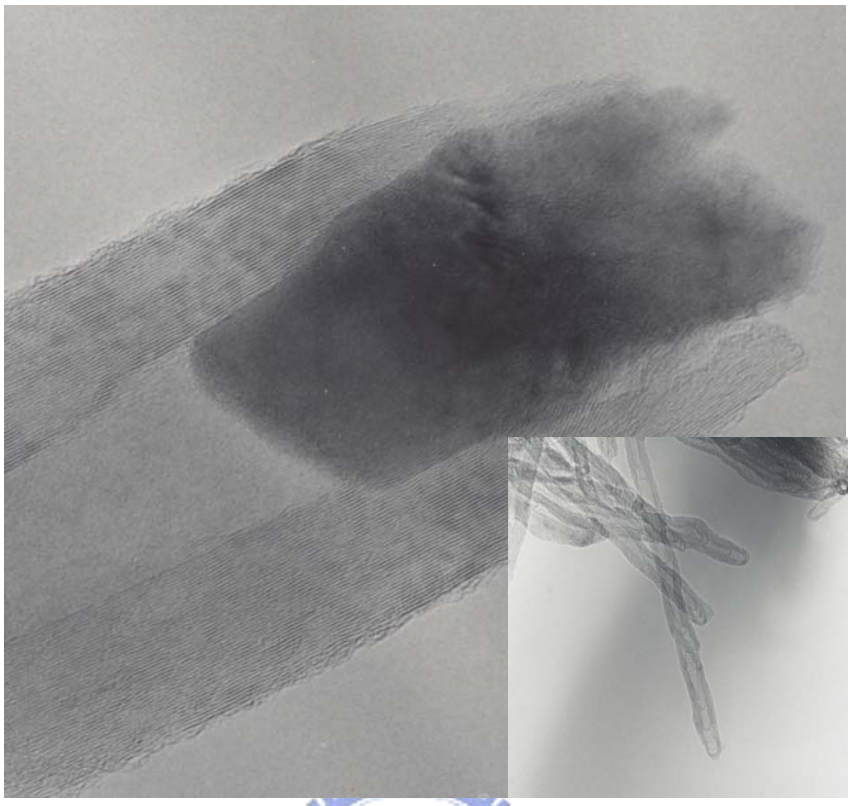

(a)

(b)

Figure 6-6 TEM images of CNTs (a) before and (b) after O_2 plasma post-treatment. The plasma power and treatment time were 400 W and 60 s, respectively.

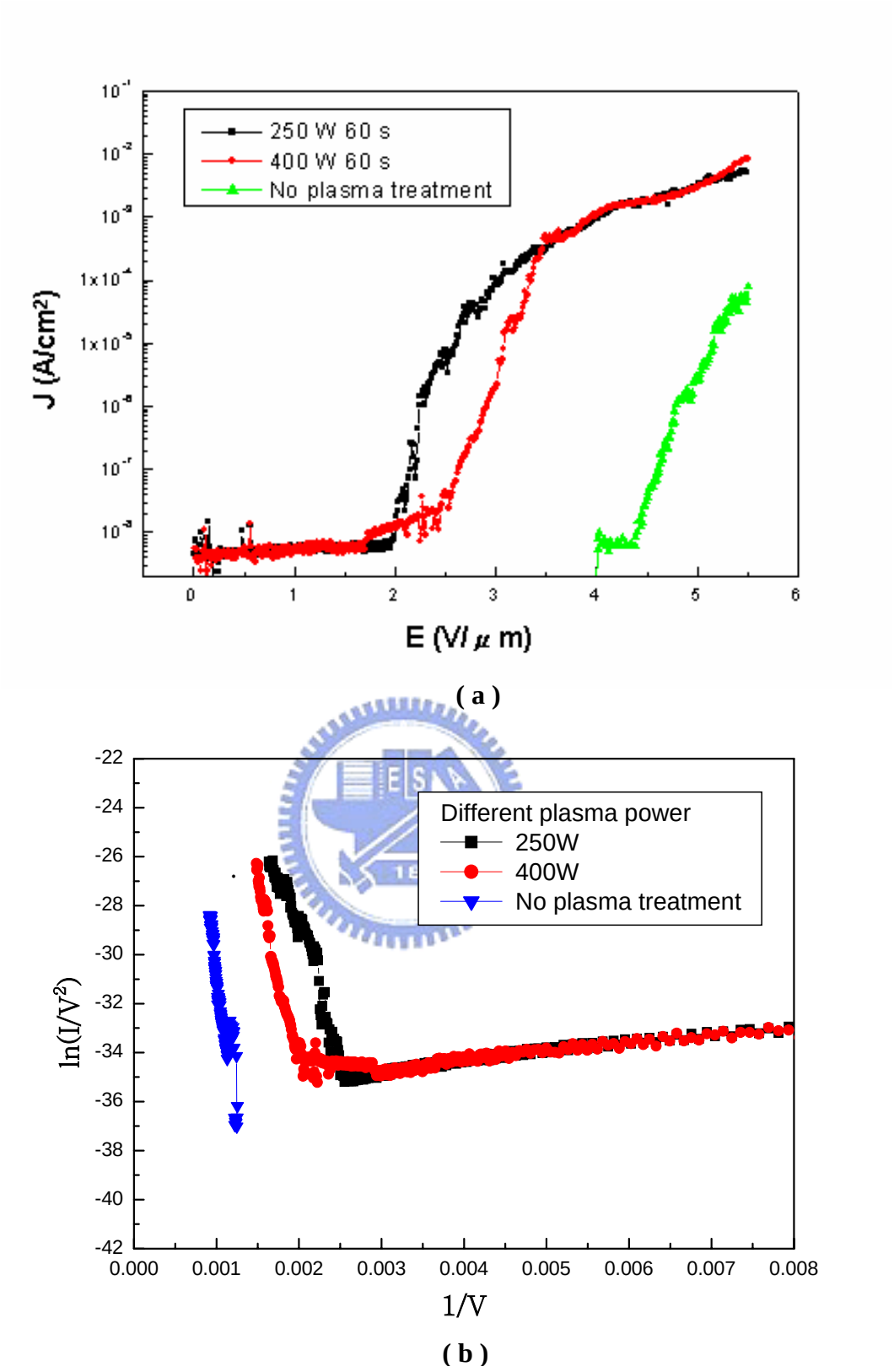

Figure 6-7 (a) Characteristics of emission current density (J) vs applied electric field (E) for CNTs with different RF plasma power treatments. The plasma etching time is 60 s. (b) corresponding FN plots.

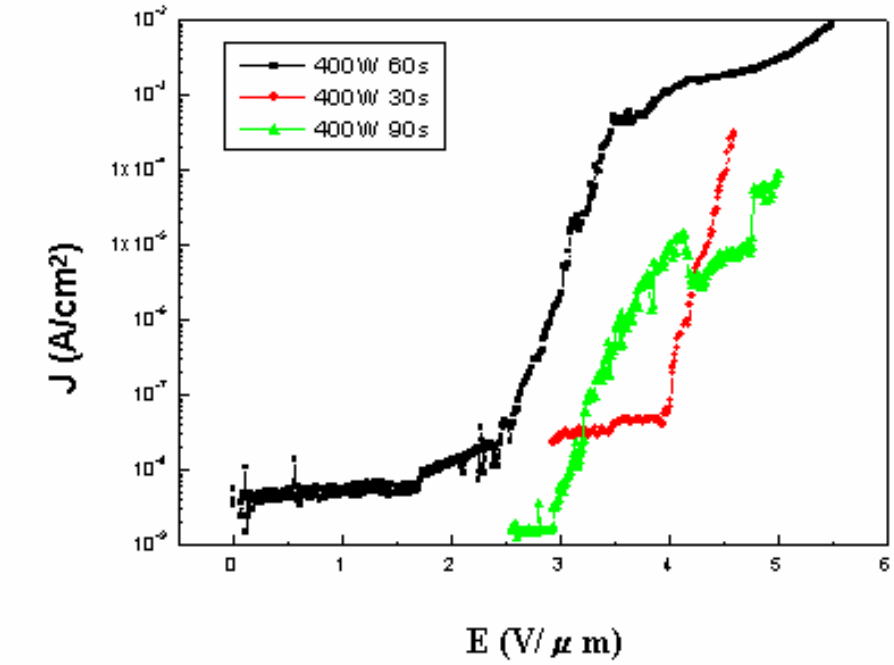

Figure 6-8 Characteristics of emission current density (J) vs applied electric field (E) for CNTs with different etching times, but constant RF power at 400 W.

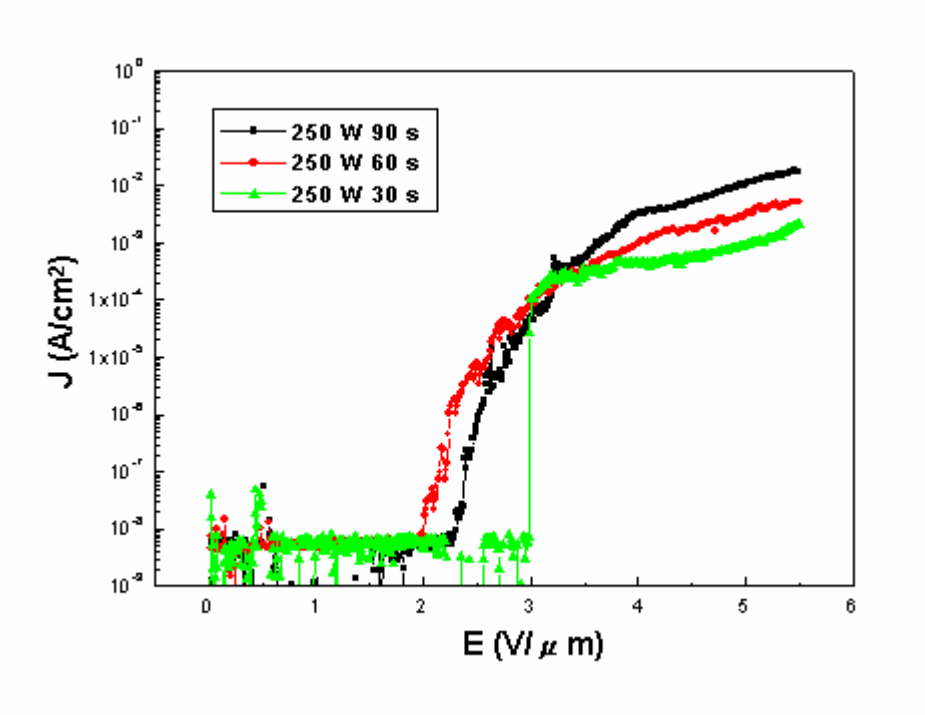

Figure 6-9 Characteristics of emission current density (J) vs applied electric field (E) for CNTs with different etching times, but constant RF power at 250 W.

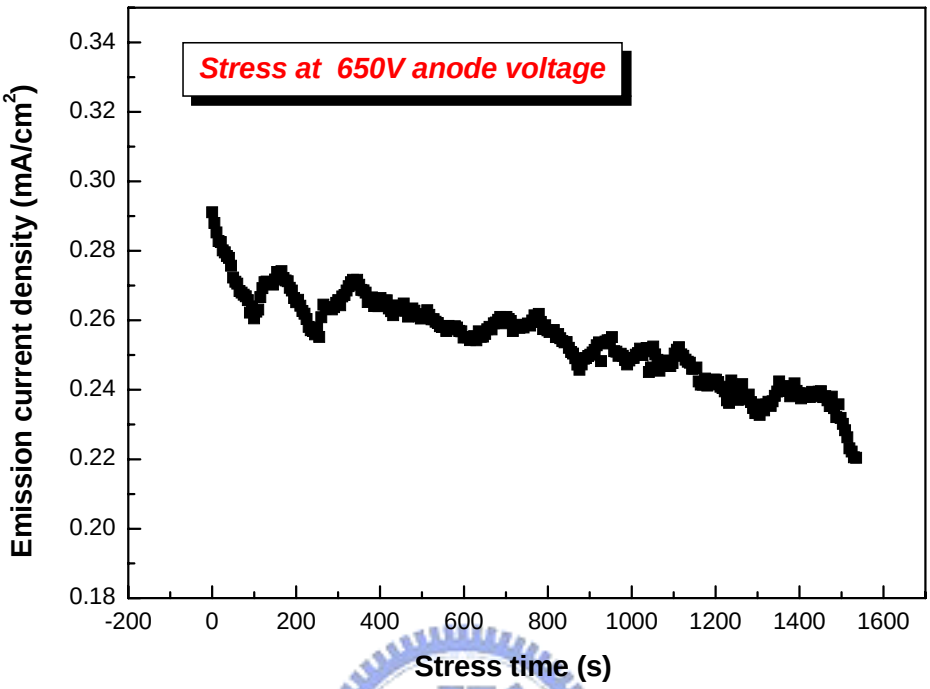

Figure 6-10 Emission current stability of CNTs after plasma treatment over period of 1500 s. The RF power was kept at 400 W and the plasma etching time was 60 s.

Table 6-1 Field emission characteristics of CNTs under different conditions of plasma post-treatment.

	Turn-on field (V/μm)	Current density J (E=5.5 V/μm)
Untreated	4.8	78.7 uA/cm^2
400 W and 30 s	4.2	0.47 mA/cm^2
400 W and 60 s	2.9	8 mA/cm^2
400 W and 90 s	3.4	87 uA/cm^2
250 W and 30 s	3.1	2.1 mA/cm^2
250 W and 60 s	2.2	4.93 mA/cm^2
250 W and 90 s	2.5	18 mA/cm^2